IEEE Access
Multidisciplinary ⋮ Rapid Review ⋮ Open Access Journal

Received August 13, 2021, accepted September 4, 2021, date of publication September 9, 2021,
date of current version September 17, 2021.

Digital Object Identifier 10.1109/ACCESS.2021.3111408

Wind Speed Ensemble Forecasting Based on Deep Learning Using Adaptive Dynamic Optimization Algorithm

ABDELHAMEED IBRAHIM[1], (Member, IEEE), SEYEDALI MIRJALILI[2,3], (Senior Member, IEEE), M. EL-SAID[4,5], SHERIF S. M. GHONEIM[6], (Senior Member, IEEE), MOSLEH M. AL-HARTHI[6], TAREK F. IBRAHIM[7,8], AND EL-SAYED M. EL-KENAWY[9,10], (Member, IEEE)

[1]Computer Engineering and Control Systems Department, Faculty of Engineering, Mansoura University, Mansoura 35516, Egypt
[2]Centre for Artificial Intelligence Research and Optimization, Torrens University Australia, Fortitude Valley, QLD 4006, Australia
[3]Yonsei Frontier Lab, Yonsei University, Seoul 03722, South Korea
[4]Electrical Engineering Department, Faculty of Engineering, Mansoura University, Mansoura 35516, Egypt
[5]Delta Higher Institute of Engineering and Technology (DHIET), Mansoura 35111, Egypt
[6]Electrical Engineering Department, College of Engineering, Taif University, Taif 21944, Saudi Arabia
[7]Department of Mathematics, Faculty of Sciences and Arts (Mahayel), King Khalid University, Abha 62529, Saudi Arabia
[8]Department of Mathematics, Faculty of Science, Mansoura University, Mansoura 35516, Egypt
[9]Department of Communications and Electronics, Delta Higher Institute of Engineering and Technology (DHIET), Mansoura 35111, Egypt
[10]Faculty of Artificial Intelligence, Delta University for Science and Technology, Mansoura 35712, Egypt

Corresponding authors: El-Sayed M. El-Kenawy (skenawy@ieee.org) and Abdelhameed Ibrahim (afai79@mans.edu.eg)

This work was supported by Taif University Researchers Supporting Project through Taif University, Taif, Saudi Arabia, under Grant TURSP-2020/122.

ABSTRACT The development and deployment of an effective wind speed forecasting technology can improve the safety and stability of power systems with significant wind penetration. Due to the wind's unpredictable and unstable qualities, accurate forecasting of wind speed and power is extremely challenging. Several algorithms were proposed for this purpose to improve the level of forecasting reliability. The Long Short-Term Memory (LSTM) network is a common method for making predictions based on time series data. This paper proposed a machine learning algorithm, called Adaptive Dynamic Particle Swarm Algorithm (AD-PSO) combined with Guided Whale Optimization Algorithm (Guided WOA), for wind speed ensemble forecasting. The AD-PSO-Guided WOA algorithm selects the optimal hyperparameters value of the LSTM deep learning model for forecasting of wind speed. In experiments, a wind power forecasting dataset is employed to predict hourly power generation up to forty-eight hours ahead at seven wind farms. This case study is taken from the Kaggle Global Energy Forecasting Competition 2012 in wind forecasting. The results demonstrated that the AD-PSO-Guided WOA algorithm provides high accuracy and outperforms several comparative optimization and deep learning algorithms. Different tests' statistical analysis, including Wilcoxon's rank-sum and one-way analysis of variance (ANOVA), confirms the accuracy of the presented algorithm.

INDEX TERMS Artificial intelligence, machine learning, optimization, forecasting, guided whale optimization algorithm.

I. INTRODUCTION

Due to the intermittence and unpredictability of wind power, the increasing penetration of wind power into power grids might significantly impact the safe functioning of power systems and power quality because the amount of wind energy generated is proportional to the wind speed. As a result, the development and deployment of an effective wind speed forecasting technology can be able to improve the safety and stability of power systems with significant wind penetration. Wind energy is one of the essential low-carbon energy technologies. It can deliver a long-term energy supply and serves as a core component for micro-grids as part of intelligent grid architecture [1].

The associate editor coordinating the review of this manuscript and approving it for publication was Dipankar Deb.

TABLE 1. Recent wind power prediction methods.

Ref.	Algorithm	Datasets	Data Size	Sampling rate
Marcos et al. 2017 [5]	Kalman filter, Statistical regression	Palmas and RN05 wind farms in Brazil	7 and 12 months	10 min
Liu et al., 2017 [6]	BPNN, RBFNN and LSSVM	Sixteen MW wind farm in Sichuan, China	2 months	15 min
Bilal et al., 2018 [14]	MLP	Four sites in Senegal.	6-9 months	1 and 10 min
Wang et al., 2018 [15]	ELM optimised by MODA	Two sites of observation in Penglai, China	37 days	10 min
Hong et al. 2019 [16]	CNN, RBFNN, DGF	Historical power data of a wind farm in Taiwan	12 months	60 min
Zhang et al., 2019 [17]	LSTM, Gaussian Mixture Model (GMM)	A 123 units wind farm in north China	3 months	15 min
Khodayar et al., 2019 [7]	IPDL, IDBN, Boltzmann Machines, Rough Set	A wind site in Colorado, US	3 years	10 min
Khodayar et al., 2019 [9]	GCDLA, LSTM, Rough Set	145 wind sites in Northern States, US	6 years	5 min
Lin et al., 2020 [3]	Isolation Forest (IF), Deep learning NN	A wind turbine SCADA data in Scotland	12 months	1 s
	IF, feed-forward NN	Seven MW wind turbine in Scotland	12 months	1 s
Jalali et al., 2021 [10]	LSTM, Enhanced grasshopper optimization algorithm	Two wind stations in Las Vegas and Denver, US	12 months	30 min

However, wind power generation is stochastic and intermittent, posing several hurdles to its widespread adoption. With the aid of wind speed and power generation projections, it is possible to reduce energy balancing and make power generating scheduling and dispatch choices. In addition, forecasts can reduce costs involved by mini missing the demand for wind curtailments and, as a result, enhancing income in power market operations. Due to the wind's unpredictable and unstable qualities, however, accurate forecasting wind speed and power is extremely difficult. A wind power forecast predicts the projected output of one or more wind turbines, often known as a wind farm. When one talks about production, it usually refers to the amount of power that a wind farm can generate (with unit's kW or MW depending on the nominal capacity of the wind farm). By combining power production throughout each period, forecasts may also be stated in energy [2].

Offer essential information about the projected wind speed and power over the next several minutes, hours, or days is the primary purpose of forecasting wind speed and power. The prediction can be separated based on power system operation requirements into four distinct time frames: long-term (from one day to seven days), medium-term (from six hours to twenty-four hours), short-term (from thirty minutes to six hours), and extremely short-term (from few seconds to thirty minutes. Turbine control and load tracking are based on very short-term estimates. Preload sharing is based on the short-term forecast. The medium-term projections are used for power system management and energy trading. Maintenance schedules for wind turbines are based on long-term forecasts [3].

Wind speed is considered a non-linear and time-relevant forecasting problem. This encourages researchers to make use of the knowledge included in the wind's historical data. Based on time-series data, one of the common methods for making predictions is the long short-term memory (LSTM) network [4]. Marcos *et al.* in [5] addressed the problem of wind power forecasting based on statistical and numerical weather prediction model models. Two different areas in Brazil were Brazilian developments on the regional atmospheric modeling system is employed to simulate forecasts of seventy-two hours ahead of the wind speed, at every ten minutes.

Liu *et al.* in [6] employed backpropagation neural network (BPNN), least squares support vector machine (LSSVM), and radial basis function NN (RBFNN) methods to forecast a sixteen MW wind farm that is located in Sichuan, China, based on two months data size at fifteen minutes sampling rate. Recently, Lin *et al.* in [3] applied Isolation Forest (IF) and deep learning NN for SCADA data of a wind turbine in Scotland to address the problem of wind power forecasting based on data size of twelve months and one-second sampling rate. Another method based on IF and feed-forward NN is applied to a seven MW wind turbine in Scotland (ORE Catapult) using a data size of twelve months and a one-second sampling rate.

To capture the wind speed data's unsupervised temporal features, an interval probability distribution learning (IPDL) model based on rough set theory and restricted Boltzmann machines was proposed in [7]. To capture the wind speed time series data's probability distribution, the IPDL model had a set of interval latent variables which can be tuned. For the future wind speed values' supervised regression, a real-valued interval deep belief network (IDBN) was also designed based on a fuzzy type II inference system and the IPDL model. Khodayar *et al.* [8] proposed a deep neural network (DNN) architecture based on stacked auto-encoder (SAE) and stacked denoising auto-encoder (SDAE) for wind speed forecasting using short-term and ultra-short-term. The auto-encoders (AEs) are used by the authors in [8] for the unsupervised feature learning from the unlabeled data of the wind. In addition, a supervised regression layer was employed for wind speed forecasting at the top of the AEs.

Authors in [9] proposed a scalable graph convolutional deep learning (GCDL) architecture to learn the powerful Spatio-temporal features in the neighboring wind farms from data of wind direction and speed. The GCDL architecture leveraged the extracted temporal features to forecast the whole graph nodes' wind-speed time series. The rough set theory was incorporated with the GCDL architecture in their model. Authors in [10] proposed a framework based on an enhanced grasshopper optimization algorithm for optimizing the hyperparameters and architecture of the LSTM deep learning model for wind speed forecasting. Table 1 shows the recent wind power prediction methods.

Hybrid machine intelligence techniques were proposed recently in the literature for wind forecasting based on different models. Authors in [11] utilized various variants of Support Vector Regression (SVR) and wavelet transform to forecast short-term wind speed. They evaluated their

proposed techniques using various performance indices to get the best regressor for wind forecasting applications. A hybrid technique was presented in [12] using learning algorithms such as Twin SVR (TSVR), Convolutional neural networks (CNN), and random forest, in addition to, discrete wavelet transform (DWT) for wind forecasting. The extracted features from wind speed in their work were enhanced based on the wavelet transform. Another hybrid technique was proposed for the anomaly detection problem for wind turbine gearbox in [13] using adaptive threshold and twin SVM (TWSVM) methods.

In this work, a dataset of wind power forecasting is tested as a case study from Kaggle Global Energy Forecasting Competition 2012-Wind Forecasting for predicting hourly power generation up to forty-eight hours ahead at seven different wind farms. A proposed adaptive dynamic particle swarm algorithm (AD-PSO) with a guided whale optimization algorithm (Guided WOA) improves the forecasting performance by enhancing the parameters of the LSTM classification method. The proposed AD-PSO-Guided WOA algorithm selects the value of the optimal hyperparameter of the LSTM deep learning model for forecasting purposes of wind speed. A binary-based AD-PSO-Guided WOA algorithm is used for the feature selection problem from the wind power forecasting dataset. The evaluation of the binary AD-PSO-Guided WOA algorithm is presented compared to Grey Wolf Optimizer (GWO) [18], Particle Swarm Optimization (PSO) [19], Stochastic Fractal Search (SFS) [20], WOA [21], [22], Genetic Algorithm (GA) [23], and Firefly Algorithm (FA) [24]. The optimized ensemble method based on the proposed algorithm is tested on the dataset. The results of this scenario are compared with Neural Networks (NN), Random Forest (RF), LSTM, Average ensemble, and k-Nearest Neighbors (k-NN) ensemble-based methods.

The AD-PSO-Guided WOA algorithm ensemble model is compared with other optimization techniques including PSO [19], WOA [22], GA [23], GWO [18], Harris Hawks Optimization (HHO) [25], [26], Slime Mould Algorithm (SMA) [27], Marine Predators Algorithm (MPA) [28], and Chimp Optimization Algorithm (ChOA) [29]. The AD-PSO-Guided WOA algorithm ensemble model is also compared with other deep learning techniques including Time delay neural network (TDNN) [30], Deep Neural Networks (DNN) [31], Stacked Denoising Autoencoder (SAE) [32], and Bidirectional Recurrent Neural Networks (BRNN) [33]. The statistical analysis of different tests is performed to confirm the accuracy of the algorithm, including a one-way analysis of variance (ANOVA) and Wilcoxon's rank-sum. The contributions of this work are summarized as follows.

- An adaptive dynamic PSO with guided WOA algorithm (AD-PSO-Guided WOA) is suggested.
- A binary AD-PSO-Guided WOA algorithm is tested for the feature selection problem using the wind power forecasting dataset.
- Tests of one-sample t-test and ANOVA are used to evaluate the binary AD-PSO-Guided WOA algorithm's statistical difference.
- To improve the wind power forecasting accuracy, an optimized ensemble method using the AD-PSO-Guided WOA algorithm is proposed.
- Wilcoxon's rank-sum and ANOVA tests are used for evaluating the proposed optimizing ensemble method's statistical difference.
- The current work's importance is applying a new optimization algorithm to enhance LSTM classifier parameters.
- The proposed algorithms can be generalized and tested for other datasets.

II. PRELIMINARIES

A. MACHINE LEARNING

1) NEURAL NETWORKS (NNs)

Artificial neural networks (ANNs) are a type of prediction model and classification approach. ANN is used to simulate complicated relationships of finding data patterns or cause-and-effect variable sets. Transient detection, approximation, time-series prediction, and pattern recognition are just a few of the disciplines they may use. ANN is considered an information processing pattern that functions similarly to the human brain. This information processing system comprises highly linked processing pieces called neurons that work together to solve issues in tandem. When formulating an algorithmic solution, a neural network comes in handy and where it is necessary to extract the structure from existing data [34].

A Multilayer perceptron (MLP) has input, output and one hidden layer. The weighted sum for the node output value is computed as follows [35].

$$S_j = \sum_{i=1}^{n} w_{ij} I_i + \beta_j \tag{1}$$

where I_i represents an input variable i, the weight of connection between neuron j and input I_i is represented as w_{ij}. The β_j parameter is a bias value. Based on using of the sigmoid activation function, the node j output is calculated as

$$f_j(S_j) = \frac{1}{1 + e^{-S_j}} \tag{2}$$

where the value of $f_j(S_j)$ is then used to get the network output as follows.

$$y_k = \sum_{j=1}^{m} w_{jk} f_j(S_j) + \beta_k \tag{3}$$

where the weights between output node k and neuron j in the hidden layer is defined as w_{jk} and β_k indicates the output layer bias value.

2) RANDOM FOREST (RF)

As a method based on statistical learning theory, random forests provide several advantages, including fewer

configurable parameters, higher prediction precision, and improved generalization ability. It extracts numerous samples from the original sample using the bootstrap sampling approach, builds decision tree modeling based on each bootstrap sample, combines the predictions of multiple decision trees, and uses a voting mechanism to determine the outcome.

For the RF training algorithm, the regression/classification tree f_b is trained based on X_b and Y_b training examples for $X = x_1, \ldots, x_n$ and $Y = y_1, \ldots, y_n$. For B times, let $b = 1, \ldots, B$. After the process of training, the unseen samples predictions x' is calculated by averaging all the predictions of individual regression trees on x' as in equation 4.

$$\hat{f} = \frac{1}{B}\sum_{b=1}^{B} f_b(x') \tag{4}$$

3) K-NEAREST NEIGHBORS (K-NN)

The model's interpretability. The findings of the prediction algorithm using the k-nearest neighbor's technique are based on the previous events that are the most like the current state based on a given distance metric. A simple average of the output values of the k nearest neighbors, or any weighted averaging, is used to make predictions. Thus, experts can analyze the findings of the k-nearest neighbor's method. The object's predictable variable in the k-NN numerical prediction this number is the average of its k closest neighbors' values. The k-NN method is one of the basic and the most powerful machine learning algorithms.

The k-NN model employs a similarity measure, Euclidean distance, to compare the data. Between x_{train} as training data and x_{test} as testing data, calculations of the Euclidean distance are based on the following equation.

$$D\left(x_{train,i}, x_{test,i}\right) = \sqrt{\sum_{i=1}^{k}(x_{train,i} - x_{test,i})^2} \tag{5}$$

To predict the output variables, k-NN determines k training data close to testing data. For unknown testing data to be predicted, the k training data output value is determined to be the nearest neighbours. The following formula is applied for predicting the testing data.

$$\hat{y} = \sum_{j=1}^{k} w_j y_j \tag{6}$$

where the jth neighbor weight is indicated as w_j and it is adjusted by the observed data, for $w_j = j/n$, for n indicates number of training data. This model can be used as a k-NN time series model.

B. DEEP LEARNING

1) LONG SHORT TERM MEMORY (LSTM)

The LSTM model is an improvement ANN model and it can be applied for different kinds of problems as discussed in [36]. The LSTM's main advantage is that it can remember the information for a long time. The LSTM architecture is shown in Figure 1. The first step of the LSTM model is to decide what kind of data from the cell state should be discarded. A forget gate layer or sigmoid layer is used for that as presented in equation 7.

$$f_t = \sigma(b_f + W_f[h_{t-1}, x_t]) \tag{7}$$

The following step is to decide about the new data to be stored in the cell state. The sigmoid layer decides about the values that need an update, and the new candidate is added to the generated state by the tanh layer as presented in equations 8 and 9.

$$i_t = \sigma(b_i + W_i[h_{t-1}, x_t]) \tag{8}$$

$$C'_t = \tanh(b_i + W_i[h_{t-1}, x_t]) \tag{9}$$

The C_{t-1} parameter, old cell state, is then updated into the C_t parameter, new cell state, by equation 10 using equations 7, 8, and 9.

$$C_t = i_t \times C'_t + f_t \times C_{t-1} \tag{10}$$

The final step is about the output decision. The sigmoid layer helps in deciding which cell state parts should be moved to output. The cell state will then use tanh and force values between [-1,1] and then multiply it with the sigmoid gate output as presented in equation 11.

$$h_t = o_t \times \tanh(C_t), \quad o_t = \sigma(b_o + W_o[h_{t-1}, x_t]) \tag{11}$$

C. ENSEMBLE TECHNIQUES

The goal such approaches is to combine the capabilities of a variety of single base models to create a predictive model. This concept can be implemented in a variety of ways. For instance, key strategies rely on resampling the training set, while others rely on alternative prediction methods or modifying some predictive technique parameters. Finally, the result of each prediction is combined using an ensemble of approaches.

III. PROPOSED ADAPTIVE DYNAMIC PSO-GUIDED WOA ALGORITHM

This section discusses the presented AD-PSO-Guided WOA algorithm using adaptive dynamic technique, particle swarm algorithm, and modified whale optimization algorithm. Algorithm (1) shows the AD-PSO-Guided WOA algorithm.

A. ADAPTIVE DYNAMIC TECHNIQUE

After the initialization of the optimization algorithm and for each solution in the population, a fitness value is evaluated. For the best fitness value, the optimization algorithm then gets the relevant best agent (solution). To start the adaptive dynamic process, the optimization algorithm starts to split agents of the population into two different groups, as in Fig. 2. The two groups are named exploitation group and exploration group. The main target of the individuals in the exploitation group is to move toward the optimal or best solution, and the main target of the individuals in the exploration group is to search the area around the leaders. The change (update)

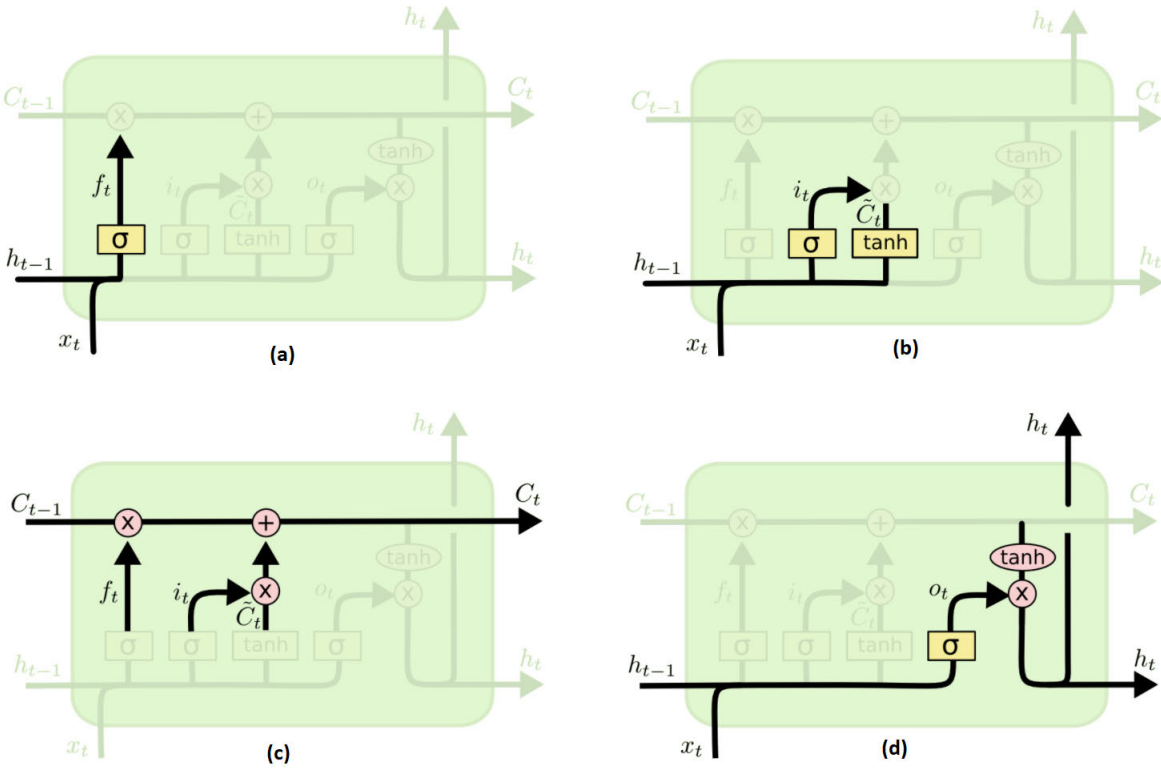

FIGURE 1. LSTM neural network architecture.

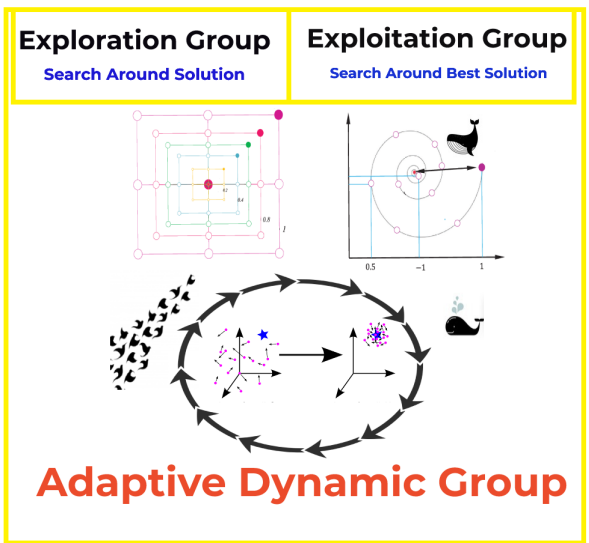

FIGURE 2. Balancing of exploration and exploitation groups in the AD-PSO-Guided WOA algorithm.

between the agents of the population groups is working in a dynamic manner. To achieve a balance between the exploitation group and exploration group, the optimization algorithm is initiated with a (50/50) population. Figure 3 explains the balancing and the dynamic change between the number of agents (individuals) in the two groups over different iteration until getting the best or optimal solution.

B. GUIDED WOA ALGORITHM

The WOA algorithm shows its advantages for different problems in the area of optimization. WOA is considered in the literature as one of the most effective optimization algorithms [20], [37]. However, it might suffer from a low capability of exploration [38]. For mathematical calculations, let's consider n to be the dimension or number of variables of the search space that whales will swim in. If it is considered that the agents (solutions) positions in the space search will be updated over time, the best solution of food will be found.

The following equation can be used in the WOA algorithm for the purpose of updating agents' positions.

$$\vec{X}(t+1) = \vec{X}^*(t) - \vec{A}.\vec{D}, \vec{D} = |\vec{C}.\vec{X}^*(t) - \vec{X}(t)| \tag{12}$$

where $\vec{X}(t)$ term represents a solution at an iteration t. The $\vec{X}^*(t)$ term represents the food or the optimal solution position. The "." indicated in this equation a kind of pairwise multiplication. The $\vec{X}(t+1)$ represents the changed agent position. The two vectors of $\vec{A}$ and $\vec{C}$ will be updated during iterations as $\vec{A} = 2\vec{a}.r_1 - \vec{a}$ and $\vec{C} = 2.r_2$. The

Algorithm 1 The AD-PSO-Guided WOA Algorithm

Initialize population $\overrightarrow{X}_i(i = 1, 2, \ldots, n)$ with size n, maximum iterations Max_{iter}, fitness function F_n.
Initialize parameters $\overrightarrow{a}$, $\overrightarrow{A}$, $\overrightarrow{C}$, l, $\overrightarrow{r_1}$, $\overrightarrow{r_2}$, $\overrightarrow{r_3}$, $\overrightarrow{w_1}$, $\overrightarrow{w_2}$, $\overrightarrow{w_3}$, $t = 1$
Evaluate fitness function F_n for each $\overrightarrow{X}_i$
Find best individual $\overrightarrow{X^*}$
while $t \leq Max_{iter}$ **do**
  if $(t\%2 == 0)$ **then**
    for $(i = 1 : i < n + 1)$ **do**
      if $(\overrightarrow{r_3} < 0.5)$ **then**
        if $(|\overrightarrow{A}| < 1)$ **then**
          Update current search agent position as $\overrightarrow{X}(t+1) = \overrightarrow{X}^*(t) - \overrightarrow{A}.\overrightarrow{D}$
        else
          Select three random search agents $\overrightarrow{X}_{rand1}$, $\overrightarrow{X}_{rand2}$, and $\overrightarrow{X}_{rand3}$
          Update $(\overrightarrow{z})$ by the exponential form of $\overrightarrow{z} = 1 - \left(\frac{t}{Max_{iter}}\right)^2$
          Update current search agent position as $\overrightarrow{X}(t+1) = \overrightarrow{w_1} * \overrightarrow{X}_{rand1} + \overrightarrow{z} * \overrightarrow{w_2} * (\overrightarrow{X}_{rand2} - \overrightarrow{X}_{rand3}) + (1 - \overrightarrow{z}) * \overrightarrow{w_3} * (\overrightarrow{X} - \overrightarrow{X}_{rand1})$
        end if
      else
        Update current search agent position as $\overrightarrow{X}(t+1) = \overrightarrow{D}'.e^{bl}.cos(2\pi l) + \overrightarrow{X}^*(t)$
      end if
    end for
    Calculate fitness function F_n for each $\overrightarrow{X}_i$ from Guided WOA
  else
    Calculate fitness function F_n for each $\overrightarrow{X}_i$ from PSO
  end if
  Update $\overrightarrow{a}$, $\overrightarrow{A}$, $\overrightarrow{C}$, l, $\overrightarrow{r_3}$
  Find best individual $\overrightarrow{X^*}$
  Set t = t + 1
end while
return $\overrightarrow{X^*}$

$\overrightarrow{a}$ term will be changed linearly from 2 (maximum value) to 0 (minimum value). The values of r_1 and r_2 are changing randomly between [0, 1].

The term Guided WOA, in this work, indicates a modified version of the original WOA algorithm [37]. In Guided WOA, the drawback of the original WOA is alleviated by updating the search strategy through one agent. The modified algorithm moves the agents toward the prey or best solution based on more than one agent. Equation 12 in the original WOA algorithm forces agents to move randomly around each other to get the global search. In the Guided WOA algorithm, however, the exploration process is enhanced by forcing agents to follow three random agents instead of one. For forcing agents not to be affected by one leader position to get more exploration, equation 12 can be replaced by the following one.

$$\overrightarrow{X}(t+1) = \overrightarrow{w_1} * \overrightarrow{X}_{rand1} + \overrightarrow{z} * \overrightarrow{w_2} * (\overrightarrow{X}_{rand2} - \overrightarrow{X}_{rand3}) + (1 - \overrightarrow{z}) * \overrightarrow{w_3} * (\overrightarrow{X} - \overrightarrow{X}_{rand1}) \quad (13)$$

where the three random solutions are represented in this equation by $\overrightarrow{X}_{rand1}$, $\overrightarrow{X}_{rand2}$, and $\overrightarrow{X}_{rand3}$. The $\overrightarrow{w_1}$ term value is updated in [0, 0.5]. The terms of $\overrightarrow{w_2}$ and $\overrightarrow{w_3}$ are changing in [0, 1]. Finally to smoothly the change between exploration and exploitation, the term $\overrightarrow{z}$ is decreasing exponentially instead of linearly and is calculated as follows.

$$\overrightarrow{z} = 1 - \left(\frac{t}{Max_{iter}}\right)^2 \quad (14)$$

where iteration number is represented as t, and Max_{iter} represents the maximum number of iterations.

C. PARTICLE SWARM OPTIMIZATION

Unlike the WOA algorithm, the PSO algorithm simulates the social behaviour of a different kind of swarming pattern of flocks in nature such as birds [18]. The agents in the PSO algorithm search for the best solution or food according to the updated velocity by changing their positions. The algorithm uses particles (agents) and each agent follows these parameters:

- The term $(x^i \in R^n)$ indicates a point or position in R^n search space. The agents' positions are calculated by a fitness function.
- the term (v^i) represents velocity or rate of change of agents positions,
- The term (p^i) indicates the last best positions of the particles.

The positions and velocities of agents are updating over iterations. The positions of agents changed using the following equation.

$$x^i_{(t+1)} = x^i_{(t)} + v^i_{(t+1)} \quad (15)$$

where the new agent position is indicated as x^i_{t+1}. Updated velocity of each agent v^i_{t+1} evaluated as in the following form.

$$v^i_{(t+1)} = C_1 r_1 (p^i_{(}t) - x^i_{(t)}) + C_2 r_2 (G - x^i_{(t)}) + \omega v^i_{(t)} \quad (16)$$

where the term ω represents the inertia weight. The terms C_1 and C_2 indicate cognition and social learning factors. The G parameter represents the global best position and the values of r_1 and r_2 are within [0; 1].

D. PROPOSED ALGORITHM COMPLEXITY ANALYSIS

The AD-PSO-Guided WOA algorithm' complexity analysis is presented in this section based on Algorithm (1). Using population number indicated as n iterations number as M_t, the complexity can be defined for each part of the algorithm as

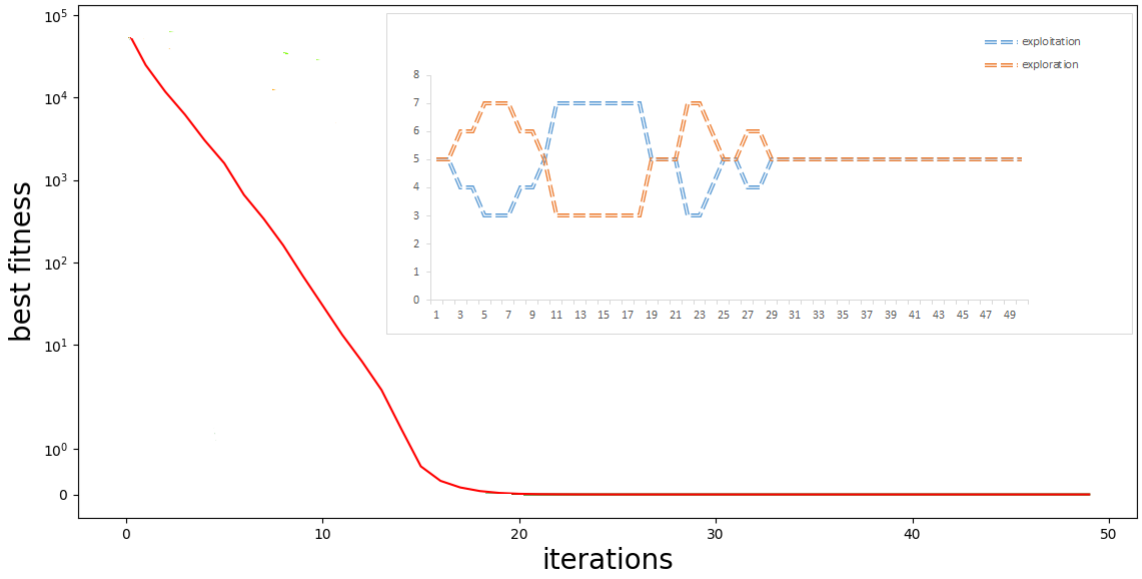

FIGURE 3. Dynamic updating of the exploration and exploitation groups in the AD-PSO-Guided WOA algorithm.

- Initializing of the population: $O\,(1)$.
- Initializing of parameters $\overrightarrow{a}$, $\overrightarrow{A}$, $\overrightarrow{C}$, l, $\overrightarrow{r_1}$, $\overrightarrow{r_2}$, $\overrightarrow{r_3}$, $\overrightarrow{w_1}$, $\overrightarrow{w_2}$, $\overrightarrow{w_3}$, $t = 1$: $O\,(1)$.
- Evaluating fitness function F_n: $O\,(n)$.
- Getting best individual $\overrightarrow{X^*}$: $O\,(n)$.
- Updating positions: $O\,(M_t \times n)$.
- Evaluating agents' fitness function using Guided WOA: $O\,(M_t \times n)$.
- Evaluating agents' fitness function using PSO: $O\,(M_t \times n)$.
- Updating parameters $\overrightarrow{a}$, $\overrightarrow{A}$, $\overrightarrow{C}$, l, $\overrightarrow{r_3}$: $O\,(M_t)$.
- Updating best solution: $O\,(M_t \times n)$.
- Increasing iteration counter: $O\,(M_t)$.

The complexity of the AD-PSO-Guided WOA algorithm can be considered as $O\,(M_t \times n)$. For m variables problems, the algorithm complexity can be considered $O\,(M_t \times n \times m)$.

E. BINARY OPTIMIZER

For the feature selection problem, the output solution should be changed to a binary solution using 0 or 1. The sigmoid function is usually employed to change the continuous solution of the optimizer to a binary solution.

$$\overrightarrow{X}_d^{(t+1)} = \begin{cases} 0 & \text{if } Sigmoid(X_{Best}) < 0.5 \\ 1 & otherwise, \end{cases}$$
$$Sigmoid(X_{Best}) = \frac{1}{1 + e^{-10(X_{Best} - 0.5)}} \tag{17}$$

where the best position is indicated as X_{Best} for t iteration. The *Sigmoid* function is used to help in changing the continuous values to be 0 or 1. For $Sigmoid(X_{Best}) \geq 0.5$, the value will change to 1, otherwise, the value will be changed to be 0.

Algorithm 2 Binary AD-PSO-Guided WOA Algorithm

1: **Initialize** AD-PSO-Guided WOA algorithm configuration, including population and parameters
2: **Change** current solutions to binary solution (0 or 1)
3: **Evaluate** fitness function and determine the best solution
4: **Train** k-NN based model and then calculate error
5: **while** $t \leq iters_{max}$ **do**
6: **Apply** AD-PSO-Guided WOA algorithm
7: **Change** updated solution to binary solution (0 or 1) based on equation 17
8: **Evaluate** fitness function for each agent
9: **Update** parameters
10: **Update** best solution
11: **end while**
12: **Return** optimal solution

Algorithm (2) shows the step by step explanation of the binary AD-PRS-Guided WOA Algorithm.

F. FITNESS FUNCTION

The solutions' quality of an optimizer is measured based on the assigned fitness function. The function is mainly depending on the error rate of classification/regression and the features that have been selected from the input dataset. The best solution is according to the set of features that can give a minimum features with a minimum classification error rate. The following equation is applied in this work for the evaluation of solutions' quality.

$$F_n = \alpha Err(O) + \beta \frac{|s|}{|f|} \tag{18}$$

where the optimizer error rate is indicated as $Err(O)$, the selected set of features is denoted as s, f represents total number of existing features. The $\alpha \in [0, 1]$, $\beta = 1 - h_1$ values are responsible of the classification error rate and the number of selected features.

IV. EXPERIMENTAL RESULTS

The experimental settings and results for wind power forecasting problems using the presented AD-PSO-Guided WOA algorithm are presented in this section. The dataset is first discussed, and then the experiments are divided into feature selection, ensemble, and comparison scenarios.

A. DATASET DESCRIPTION

A wind power forecasting dataset to predict hourly power generation up to forty-eight hours ahead at seven wind farms is tested in the experiments as a case study. The dataset is published on Kaggle as Global Energy Forecasting Competition 2012 - Wind Forecasting [39]. The presented AD-PSO-Guided WOA algorithm is applied in different scenarios to test the best available accuracy compared to algorithms in the literature. A statistical analysis of different tests is also applied to the tested dataset to show the algorithm's accuracy. Prediction of regression is shown in Fig. 4. The figure shows the actual values from the dataset and the predicted values based on the proposed AD-PSO-Guided WOA algorithm.

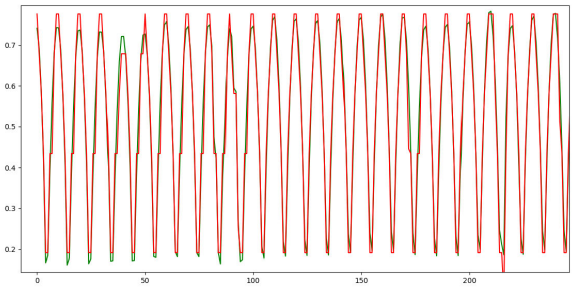

FIGURE 4. The actual (green color) and predicted (red color) values based on the AD-PSO-Guided WOA algorithm.

B. FEATURE SELECTION SCENARIO

The experiment in this scenario desired to show the feature selection efficiency by the proposed binary AD-PSO-Guided WOA algorithm. The binary AD-PSO-Guided WOA algorithm performance is compared with the binary version of GWO (bGWO) [18], binary PSO (bPSO) [19], binary SFS (bSFS) [20], binary WOA (bWOA) [21], [22], binary FA (bFA) [24], and binary GA (bGA) [23] using performance metrics shown in Table 2. The variables in Table 2 are indicated as follows. An optimizer number of runs is indicated as M, the best solution at the run number j is represented by g_j^*, size of the g_j^* vector is indicated as $size(g_j^*)$, and the number of tested points is N. A classifier's output label for a point i is C_i, a class's label for a point i is L_i, the total number of features is D, and the $Match$ function is used for calculating the matching between two inputs. The metrics include average error and standard deviation fitness.

TABLE 2. Feature selection performance metrics.

Metric	Value
Average Error	$1 - \frac{1}{M}\sum_{j=1}^{M}\frac{1}{N}\sum_{i=1}^{N} Match(C_i, L_i)$
Average Select Size	$\frac{1}{M}\sum_{j=1}^{M}\frac{size(g_j^*)}{D}$
Average Fitness	$\frac{1}{M}\sum_{j=1}^{M} g_j^*$
Best Fitness	$Min_{j=1}^{M} g_j^*$
Worst Fitness	$Max_{j=1}^{M} g_j^*$
Standard Deviation	$\sqrt{\frac{1}{M-1}\sum(g_j^* - Mean)^2}$

TABLE 3. Configuration of AD-PSO-guided WOA algorithm.

Parameter	Value
# Whales	20
# Iterations	20
# Runs	20
Dimension	# Features
Inertia W_{max}, W_{min}	[0.9,0.6]
Acceleration constants C_1, C_2	[2,2]
α of F_n	0.99
β of F_n	0.01

TABLE 4. Configuration of compared algorithms.

Algorithm	Parameter (s)	Value (s)
GWO	a	2 to 0
	# Wolves	20
	# Iterations	20
PSO	Inertia W_{max}, W_{min}	[0.9,0.6]
	Acceleration constants C_1, C_2	[2,2]
	# Particles	20
	Generations	20
SFS	Maximum diffusion level	1
WOA	a	2 to 0
	r	[0,1]
	# Whales	20
	# Iterations	20
GA	Mutation ratio	0.1
	Crossover	0.9
	Selection mechanism	Roulette wheel
	Population size	20
	Generations	20
FA	# Fireflies	10

The AD-PSO-Guided WOA algorithm configuration setting in experiments is shown in Table 3. The AD-PSO-Guided WOA algorithm's initial parameters are the number of population equal 20, the maximum number of iterations is set to 20, and the number of runs equals 20 for the dataset. The main parameters for the PSO algorithm are W_{max} and W_{min}, which their values are set to 0.9 and 0.6, respectively. In addition, the α parameter is assigned to be (0.99) and β is assigned to be $(1-\alpha)$. The GWO, PSO, SFS, WOA, FA, and GA algorithms' configuration is shown in Table 4.

In this scenario, Table 5 shows the results provided by GWO, PSO, SFS, WOA, FA, and GA algorithms. The AD-PSO-Guided WOA algorithm shows a minimum average error of (0.4790) for feature selection for the presented

TABLE 5. Results of feature selection for the presented and compared binary algorithms.

	AD-PSO-Guided WOA	bGWO	bPSO	bSFS	bWOA	bFA	bGA
Average error	0.4790	0.5047	0.5385	0.5481	0.5383	0.5369	0.5183
Average Select size	0.2320	0.4275	0.4275	0.5669	0.5909	0.4620	0.3699
Average Fitness	0.3510	0.3541	0.3525	0.3754	0.3603	0.4044	0.3655
Best Fitness	0.2521	0.2744	0.3328	0.2651	0.3244	0.3231	0.2688
Worst Fitness	0.3305	0.3413	0.4005	0.3667	0.4005	0.4207	0.3839
Standard deviation Fitness	0.1635	0.1679	0.1680	0.1742	0.1665	0.2011	0.1665

TABLE 6. Results of ANOVA test for feature selection of the presented and compared binary algorithms.

	SS	DF	MS	F (DFn, DFd)	P value
Treatment (between columns)	0.07358	6	0.01226	F (6, 133) = 11.75	P < 0.0001
Residual (within columns)	0.1387	133	0.001043	-	-
Total	0.2123	139	-	-	-

TABLE 7. One sample t-test for feature selection of the presented and compared binary algorithms.

	AD-PSO-Guided WOA	bGWO	bPSO	bSFS	bWOA	bFA	bGA
Theoretical mean	0	0	0	0	0	0	0
Actual mean	0.479	0.5022	0.5393	0.5481	0.5388	0.5352	0.519
# values	20	r20	20	20	20	20	20
One sample t-test							
t, df		t=54.41, df=19	t=72.46, df=19	t=188.9, df=19	t=210.3, df=19	t=40.08, df=19	t=92.86, df=19
P value (two tailed)		0.0001	0.0001	0.0001	0.0001	0.0001	0.0001
P value summary		****	****	****	****	****	****
Significant (alpha=0.05)?		Yes	Yes	Yes	Yes	Yes	Yes
How big is the discrepancy?							
Discrepancy		0.5022	0.5393	0.5481	0.5388	0.5352	0.519
Discrepancy SD		0.04128	0.03328	0.01298	0.01146	0.05972	0.02499
Discrepancy SEM		0.00923	0.007442	0.002902	0.002562	0.01335	0.005589
95% confidence interval		0.4829 to 0.5215	0.5237 to 0.5548	0.5420 to 0.5542	0.5334 to 0.5442	0.5073 to 0.5632	0.5073 to 0.5307
R squared		0.9936	0.9964	0.9995	0.9996	0.9883	0.9978

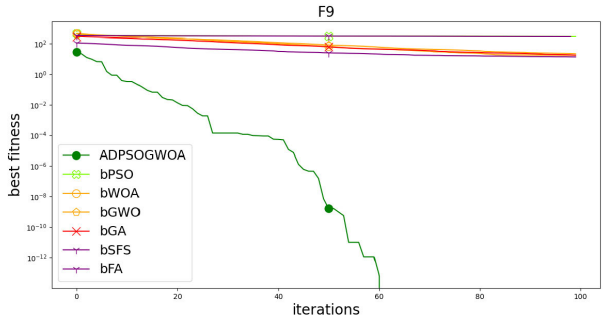

FIGURE 5. The AD-PSO-Guided WOA algorithm convergence curve compared to different algorithms.

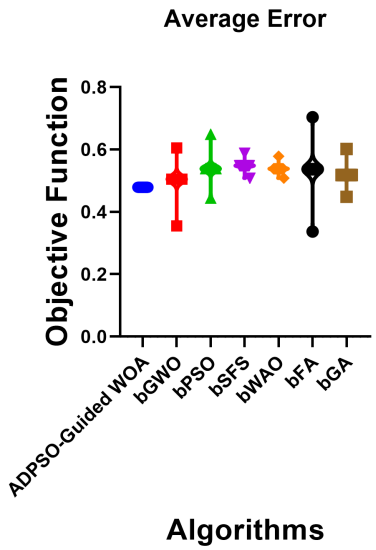

FIGURE 6. The AD-PSO-Guided WOA algorithm average error based on the objective function compared to different binary algorithms.

results. The AD-PSO-Guided WOA algorithm, based on the minimum error of the tested problem, is the best and the SFS algorithm is the worst. In terms of standard deviation, the AD-PSO-Guided WOA algorithm has the lowest value of (0.1635) which indicates the algorithm's stability and robustness.

The convergence curve of the AD-PSO-Guided WOA algorithm compared to other algorithms is shown in Figure 5. The figure shows the exploitation capability of the algorithm and its ability to avoid possible local optima that can be occurred during the optimization process. Figure 6 shows the AD-PSO-Guided WOA average error based on the objective function compared to different algorithms. The minimum, maximum, and average values for different binary algorithms indicate the advantages of the presented algorithm. The p-values of the AD-PSO-Guided WOA algorithm are tested compared to GWO, PSO, SFS, WOA, FA, and GA algorithms by ANOVA and t-test tests in Tables 6 and 7, respectively. The

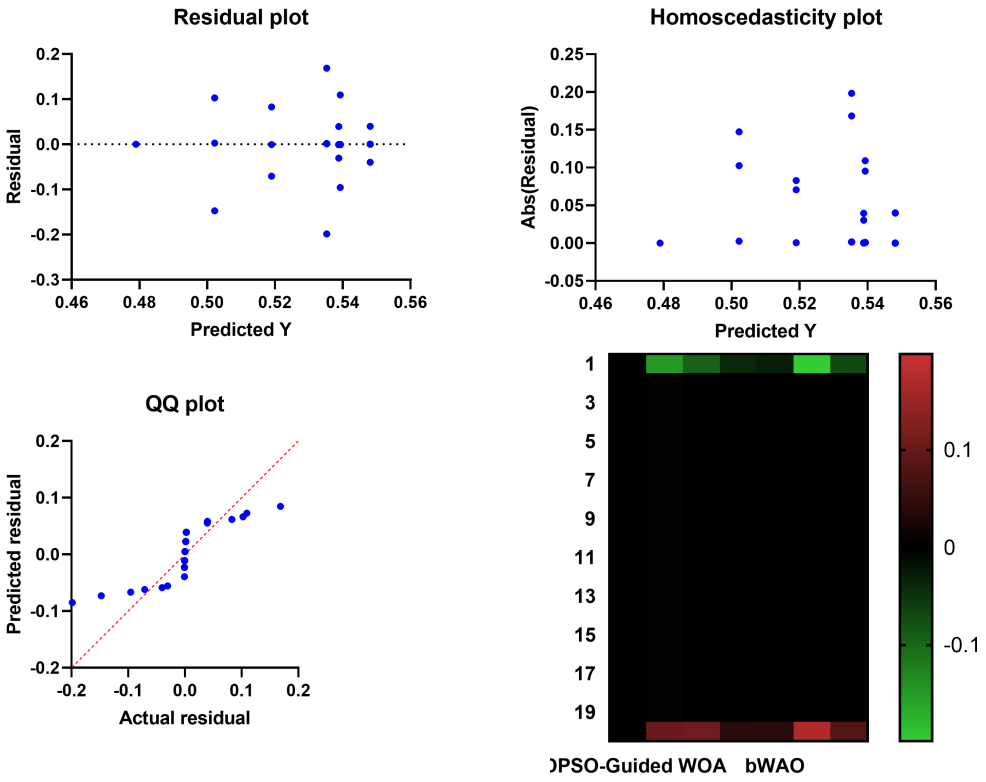

FIGURE 7. Residual, heteroscedasticity, QQ plots and heat map of the presented and compared algorithms for feature selection problem.

statistical analysis results show the superiority and statistical significance of the suggested algorithm.

The residual values and plots can be useful for some datasets that are not suitable candidates for feature selection. To achieve the ideal case, the residual values should be distributed uniformly around the horizontal axis. Considering that the sum and mean of the residuals are equal to zero, the residual value is computed as the difference between predicted and actual values. The residual plot is shown in Figure 7. A nonlinear and linear model is decided from the residual plot patterns and the appropriate one is determined. The heteroscedasticity plot is shown in Figure 7. Homoscedasticity describes if the error term is the same across the values of independent variables. Figure 7 also shows the quantile-quantile (QQ) plot, probability plot, and heat map. Since the distributions of points in the QQ plot are well fitted on the predetermined line, the actual and predicted residuals are considered to be linearly related. This confirms the presented AD-PSO-Guided WOA algorithm's performance.

C. ENSEMBLE FORECASTING SCENARIO

This scenario is formulated using ensemble-based models of the average ensemble, k-NN ensemble, and the proposed optimizing ensemble model based on the AD-PSO-Guided WOA algorithm. Some ensemble models use the training instances of the three base models of NN, RF, and LSTM. This can be used to forecast the unknown observations to predict wind speed. The hyperparameters that are fed to the AD-PSO-Guided WOA algorithm to train the LSTM model are the number of epochs T_e, size of champion attention weights subset W_a, encoding length for each attention weights L_e, and size of attention weights set N_a.

The evaluation metrics in this scenario include Root Mean Squared Error (RMSE), Relative RMSE (RRMSE), Mean Absolute Percentage Error (MAPE), Mean Absolute Error (MAE), and the correlation coefficient (r) [40]. The RMSE is calculated as follows.

$$RMSE = \sqrt{\frac{\sum_{i=1}^{n}(H_{p,i} - H_i)^2}{n}} \tag{19}$$

where predicted value is represented as $H_{p,i}$ and the H_i value represents the actual measured. The total number of values is indicated as n. The RRMSE metric is calculated as follows.

$$RRMSE = \frac{\sqrt{\frac{1}{n}\sum_{i=1}^{n}(H_{p,i} - H_i)^2}}{\sum_{i=1}^{n}(H_{p,i})} \times 100 \tag{20}$$

The MAE calculates the average amount of errors in a set of predictions and is calculated as follows.

$$MAE = \frac{1}{n}\sum_{i=1}^{n}|H_{p,i} - H_i| \tag{21}$$

TABLE 8. Different ensemble-based and single models wind speed forecasting results.

	NN	RF	LSTM	Average Ensemble	k-NN Ensemble	Optimizing Ensemble
MAPE (%)	12.8372	7.3846	6.9924	5.1134	3.6111	1.8755
MAE	0.4961	0.3163	0.2303	0.1013	0.0134	0.00476
RMSE	0.491329643	0.231488171	0.109544	0.091676794	0.01493511	0.003728832

TABLE 9. The presented optimizing ensemble model' descriptive statistics versus other models.

	NN	RF	LSTM	Average Ensemble	k-NN Ensemble	Optimizing Ensemble
# values	30	30	30	30	30	30
Minimum	0.4306	0.181	0.08629	0.07737	0.01011	0.003668
25% Percentile	0.4521	0.194	0.09462	0.08521	0.0111	0.003682
Median	0.4696	0.2405	0.1144	0.09076	0.01387	0.003715
75% Percentile	0.4934	0.2598	0.1295	0.1012	0.01712	0.003744
Maximum	0.5354	0.288	0.1403	0.1085	0.01862	0.003918
Range	0.1048	0.107	0.05401	0.0311	0.008508	0.0002499
Mean	0.4749	0.2304	0.1136	0.09341	0.01407	0.003722
Std. Deviation	0.03051	0.03408	0.01845	0.009185	0.002865	0.00004836
Std. Error of Mean	0.005571	0.006222	0.003369	0.001677	0.0005231	0.000008829
Lower 95% CI of mean	0.4635	0.2177	0.1067	0.08998	0.013	0.003704
Upper 95% CI of mean	0.4863	0.2432	0.1204	0.09684	0.01514	0.00374
Coefficient of variation	6.425%	14.79%	16.25%	9.833%	20.37%	1.299%
Geometric mean	0.474	0.2279	0.1121	0.09298	0.01378	0.003722
Geometric SD factor	1.065	1.163	1.18	1.104	1.228	1.013
Lower 95% CI of geo. mean	0.4629	0.2154	0.1053	0.08962	0.01277	0.003704
Upper 95% CI of geo. mean	0.4853	0.2412	0.1192	0.09646	0.01488	0.003739
Harmonic mean	0.4731	0.2254	0.1106	0.09254	0.01351	0.003721
Lower 95% CI of harm. mean	0.4623	0.2133	0.1041	0.08926	0.01255	0.003704
Upper 95% CI of harm. mean	0.4844	0.2391	0.118	0.09607	0.01462	0.003739
Quadratic mean	0.4758	0.2329	0.115	0.09385	0.01435	0.003722
Lower 95% CI of quad. mean	0.4641	0.22	0.108	0.09035	0.01323	0.003704
Upper 95% CI of quad. mean	0.4873	0.245	0.1216	0.09722	0.01538	0.00374
Skewness	0.5804	-0.1167	-0.0517	0.08423	0.1666	2.278
Kurtosis	-0.6107	-1.471	-1.401	-1.346	-1.438	8.546
Sum	14.25	6.913	3.407	2.802	0.422	0.1117

The MAPE is one of the most commonly used metrics to measure forecast accuracy, which is similar to MAE but normalized by true observation. MAPE can be calculated as follows.

$$MAPE = \frac{100}{n}\sum_{i=1}^{n}\frac{|H_{p,i} - H_i|}{H_{p,i}} \tag{22}$$

The next metric is the correlation coefficient r which can be calculated as follows.

$$r = \frac{\sum_{i=1}^{n}(x_i - \bar{x})(y_i - \bar{y})}{\sqrt{\sum_{i=1}^{n}(x_i - \bar{x})^2(y_i - \bar{y})^2}} \tag{23}$$

where x_i represents values of variable x in a sample and y_i represents values of variable y in a sample. $\bar{x}$ and $\bar{y}$ are the mean of the x values and y values, respectively.

Different ensemble-based and single models results are shown in Table 8. The ensemble-based models in this table show promising results than single models of NN, RF, and LSTM. The proposed optimizing ensemble model, based on the deep LSTM learning model, with RMSE of (0.003728832), MAE of (0.00476), and MAPE of (1.8755), gives noticeable results compared to the k-NN and average ensemble models. Table 9 shows the detailed descriptive statistics of the presented optimizing ensemble model versus other models. Figure 8 shows the curves of Receiver Operating Characteristics (ROC) for the proposed optimizing ensemble model and the compared models. These figures indicated that the proposed ensemble model distinguishes data with a high Area Under the Curve (AUC) value near to 1.0. The proposed optimizing ensemble algorithm stability versus the compared models are confirmed by the RMSE

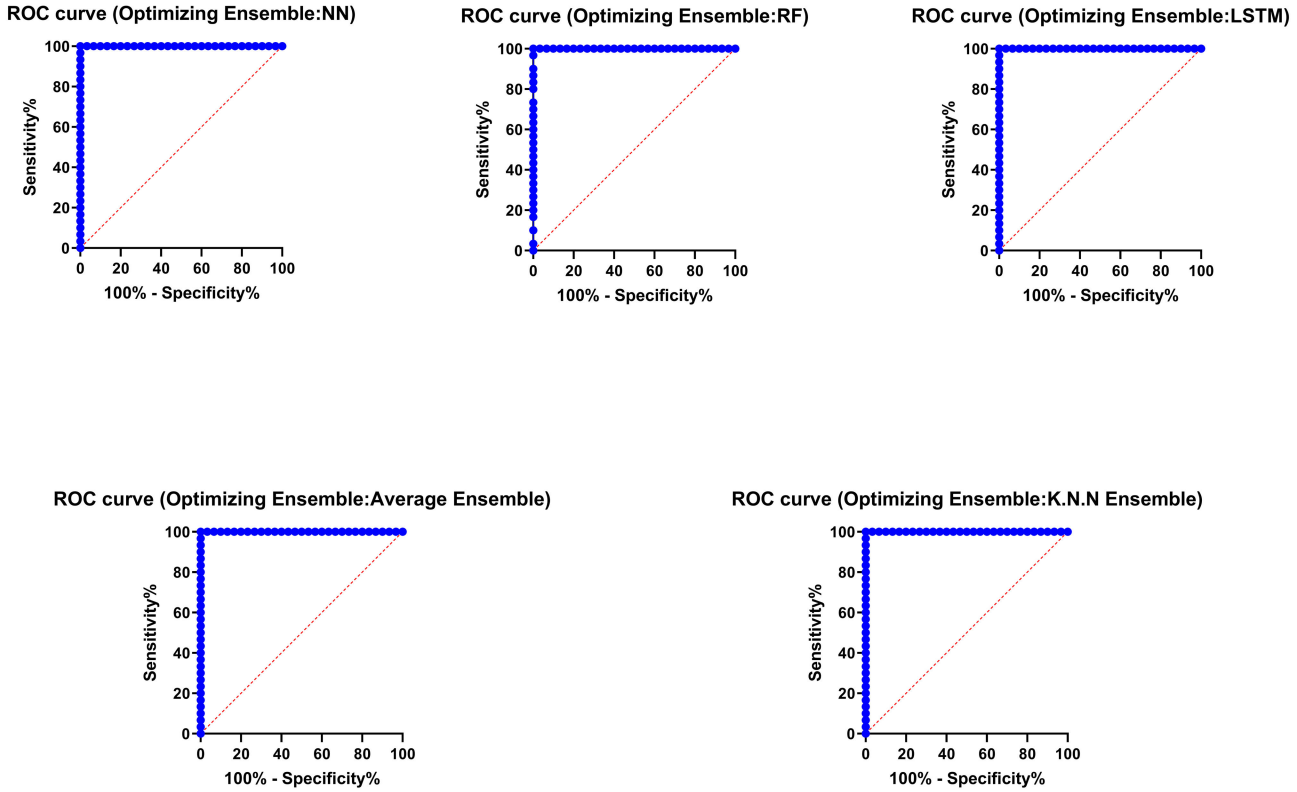

FIGURE 8. The presented optimizing ensemble model's ROC curves versus other models.

TABLE 10. ANOVA results of the base and ensemble models for the wind speed forecasting.

	SS	DF	MS	F (DFn, DFd)	P value
Between columns, Treatment	4.688	5	0.9377	F (5, 174) = 2228	P < 0.0001
Within columns, Residual	0.07323	174	0.000421	-	-
Total	4.762	179	-	-	-

TABLE 11. Wilcoxon signed rank test results of the base and ensemble models for the wind speed forecasting.

	NN	RF	LSTM	Average Ensemble	k-NN Ensemble	Optimizing Ensemble
Theoretical median	0	0	0	0	0	0
Actual median	0.4696	0.2405	0.1144	0.09076	0.01387	0.003715
# values	30	r30	30	30	30	30
Wilcoxon Signed Rank Test						
Sum of Signed ranks (W)	465	465	465	465	465	465
Positive ranks, Sum	465	465	465	465	465	465
Negative ranks, Sum	0	0	0	0	0	0
P value (two tailed)	0.0001	0.0001	0.0001	0.0001	0.0001	0.0001
Estimate or Exact?	Exact	Exact	Exact	Exact	Exact	Exact
Summary of P value	****	****	****	****	****	****
Significant (alpha=0.05)?	Yes	Yes	Yes	Yes	Yes	Yes
How big is the discrepancy?						
Discrepancy	0.4696	0.2405	0.1144	0.09076	0.01387	0.003715

distribution, shown in Figure 9, the histogram of RMSE, shown in Figure 10, the histogram of RRMSE, shown in Figure 11, and the histogram of MAPE, shown in Figure 12.

Tests of ANOVA and Wilcoxon's rank-sum are applied in this scenario to evaluate the statistical differences between the presented and compared models. ANOVA output results are shown in Table 10. Wilcoxon's rank-sum statistical analysis presented in Table 11 determines if the models' results have a significant difference. For p-value $<$ 0.05, this indicates significant superiority. The results show the AD-PSO-Guided

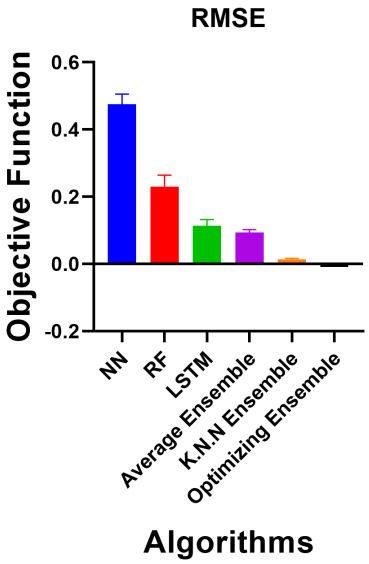

FIGURE 9. RMSE based on objective function of the presented optimizing ensemble model and other models.

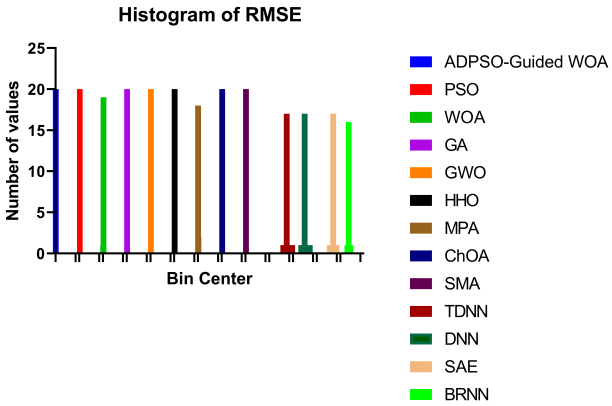

FIGURE 10. Histogram of RMSE of the presented optimizing ensemble model and other models with Bin Center range of (0.00 - 0.59) based on number of values.

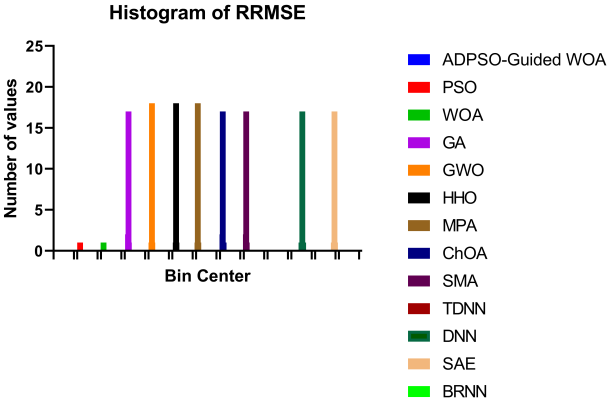

FIGURE 11. Histogram of RRMSE of the presented optimizing ensemble model and other models with Bin Center range of (1.0 - 51.5) based on number of values.

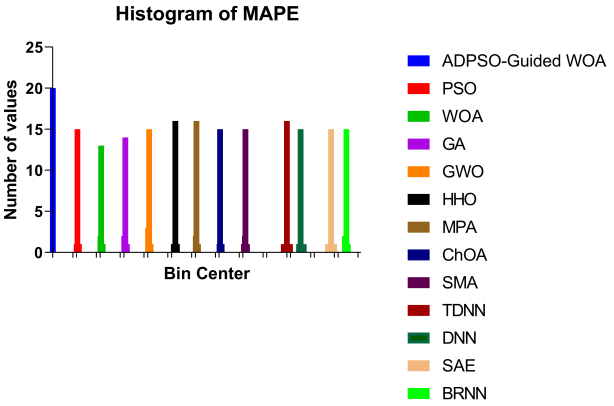

FIGURE 12. Histogram of MAPE of the presented optimizing ensemble model and other models with Bin Center range of (1.8 - 14.8) based on number of values.

WOA algorithm-based proposed ensemble model superiority and also show the algorithm's statistical significance.

The residual plot in this scenario is shown in Figure 13. The heteroscedasticity plot, QQ plot, and heat map are also shown in Figure 13. Since the distributions of points in the QQ plot are well fitted on the line, the predicted and the actual residuals are considered as linearly related which confirms the proposed AD-PSO-Guided WOA ensemble-based algorithm's performance for the wind speed forecasting problem.

D. COMPARISONS SCENARIO

The third and last scenario is designed to show the performance of the optimizing ensemble-based AD-PSO-Guided WOA algorithm compared with PSO [19], WOA [22], GA [23], GWO [18], HHO [25], [26], MPA [28], ChOA [29], and SMA [27]. The AD-PSO-Guided WOA algorithm ensemble model is also compared with four deep learning techniques including TDNN [30], DNN [31], SAE [32], and BRNN [33].

Table 12 shows the comparison results of the wind speed forecasting based on the proposed algorithm compared to other optimization techniques. The results in the table show that the presented optimizing ensemble model, based on the LSTM deep learning model and the AD-PSO-Guided WOA algorithm, gives competitive results with MAPE of (1.8755), MAE of (0.00476), RMSE of (0.003728832), RRMSE of (1.279369489), and r of (0.9998878) compared to other algorithms for the wind speed forecasting tested problem. Table 13 shows the proposed algorithm's descriptive statistics compared to other optimization techniques over 20 runs.

The ANOVA test results for wind speed forecasting based on the proposed algorithm compared to other optimization techniques is shown in Table 14. The test of the Wilcoxon Signed-Rank rest of the wind speed forecasting results based on the proposed algorithm compared to other optimization

TABLE 12. Comparison of wind speed forecasting results using the presented algorithm and other optimization techniques.

Metric	ADPSO-Guided WOA	PSO	WOA	GA	GWO	HHO	MPA	ChOA	SMA
MAPE (%)	1.8755	2.337	2.3559	2.6697	2.5574	4.1236	2.3157	2.44689	3.3312
MAE	0.00476	0.00715	0.007331	0.009123	0.008845	0.0099845	0.005089	0.007402	0.0068875
RMSE	0.003728832	0.00612567	0.006613066	0.008797	0.007802	0.009532	0.0049876	0.006675	0.0058746
RRMSE (%)	1.279369489	7.325162974	8.445619	9.985368	8.886955	10.131245	5.0124517	7.884593	6.991536
r	0.9998878	0.9977836	0.99764592	0.996771	0.997022	0.986612445	0.9945331	0.997536	0.9981303

TABLE 13. The presented algorithm's description statistics compared to other optimization techniques over 20 runs.

	ADPSO-Guided WOA	PSO	WOA	GA	GWO	HHO	MPA	ChOA	SMA
Number of values	20	20	20	20	20	20	20	20	20
Minimum	0.003429	0.005126	0.004613	0.005797	0.00598	0.006532	0.003988	0.005675	0.005075
25% Percentile	0.003729	0.006126	0.006613	0.008797	0.007802	0.009532	0.004988	0.006675	0.005875
Median	0.003729	0.006126	0.006613	0.008797	0.007802	0.009532	0.004988	0.006675	0.005875
75% Percentile	0.003729	0.006126	0.006613	0.008797	0.007802	0.009532	0.004988	0.006675	0.005875
Maximum	0.003829	0.007126	0.008613	0.009997	0.009902	0.01235	0.005988	0.008675	0.007875
Range	0.0004	0.002	0.004	0.0042	0.003922	0.005821	0.002	0.003	0.0028
10% Percentile	0.003639	0.006126	0.005713	0.006897	0.007802	0.009532	0.004988	0.00657	0.005875
90% Percentile	0.003729	0.007026	0.007513	0.008797	0.007802	0.009532	0.005888	0.007665	0.006805
Mean	0.003714	0.006176	0.006613	0.008557	0.007816	0.009523	0.005038	0.006774	0.006
Std. Deviation	0.00007452	0.000394	0.000726	0.000867	0.000638	0.000945	0.000394	0.000563	0.000534
Std. Error of Mean	0.00001666	8.81E-05	0.000162	0.000194	0.000143	0.000211	8.81E-05	0.000126	0.000119
Coefficient of variation	2.006%	6.380%	10.97%	10.13%	8.159%	9.920%	7.821%	8.314%	8.900%
Geometric mean	0.003713	0.006164	0.006574	0.008508	0.007791	0.009476	0.005023	0.006754	0.00598
Geometric SD factor	1.021	1.066	1.12	1.121	1.085	1.111	1.081	1.081	1.086
Harmonic mean	0.003712	0.006152	0.006532	0.008451	0.007766	0.009423	0.005009	0.006735	0.005962
Quadratic mean	0.003715	0.006188	0.006651	0.008599	0.007841	0.009567	0.005053	0.006796	0.006023
Skewness	-3.136	0.5305	5.71E-15	-2.126	0.6519	-0.284	0.5305	2.133	2.475
Kurtosis	12.45	4.985	5.327	5.698	9.699	9.538	4.985	7.604	8.619
Sum	0.07428	0.1235	0.1323	0.1711	0.1563	0.1905	0.1008	0.1355	0.12

TABLE 14. ANOVA test results for wind speed forecasting using the presented algorithm and other optimization techniques over 20 runs.

	SS	DF	MS	F (DFn, DFd)	P value
Between columns, Treatment	0.000502	8	6.28E-05	F (8, 171) = 161.7	P < 0.0001
Within columns, Residual	6.64E-05	171	3.88E-07	-	-
Total	0.000569	179	-	-	-

TABLE 15. Wilcoxon signed rank test of wind speed forecasting results using the presented algorithm and other optimization techniques over 20 runs.

	ADPSO-Guided WOA	PSO	WOA	GA	GWO	HHO	MPA	ChOA	SMA
Theoretical median	0	0	0	0	0	0	0	0	0
Actual median	0.003729	0.006126	0.006613	0.008797	0.007802	0.009532	0.004988	0.006675	0.005875
# Values	20	20	20	20	20	20	20	20	20
Wilcoxon Signed Rank Test									
Signed ranks (W), Sum	210	210	210	210	210	210	210	210	210
Positive ranks, Sum	210	210	210	210	210	210	210	210	210
Negative ranks, Sum	0	0	0	0	0	0	0	0	0
P value (two tailed)	0.0001	0.0001	0.0001	0.0001	0.0001	0.0001	0.0001	0.0001	0.0001
Estimate or Exact?	Exact	Exact	Exact	Exact	Exact	Exact	Exact	Exact	Exact
P value summary	****	****	****	****	****	****	****	****	****
Significant (alpha=0.05)?	Yes	Yes	Yes	Yes	Yes	Yes	Yes	Yes	Yes
How big is the discrepancy?									
Discrepancy	0.003729	0.006126	0.006613	0.008797	0.007802	0.009532	0.004988	0.006675	0.005875

techniques is also shown in Table 15. The results confirm the superiority of the AD-PSO-Guided WOA based proposed ensemble model and indicate the statistical significance of the algorithm for the wind speed forecasting tested problem compared to the PSO, WOA, GA, and GWO algorithms.

Table 16 shows the comparison results of the wind speed forecasting based on the proposed algorithm compared to

TABLE 16. Comparison of wind speed forecasting results using the presented algorithm and other deep learning techniques.

	ADPSO-Guided WOA	TDNN	DNN	SAE	BRNN
MAPE (%)	1.8755	14.7615	8.1996	12.6632	7.113
MAE	0.00476	0.5377	0.3316	0.4991	0.3226
RMSE	0.003728832	0.5126012	0.3371776	0.478634	0.244604
RRMSE (%)	1.279369489	52.659735	27.887544	48.75756	22.4404
r	0.9998878	0.8766512	0.8963578	0.887633	0.909132

TABLE 17. The presented algorithm's description statistics compared to other deep learning techniques over 20 runs.

	ADPSO-Guided WOA	TDNN	DNN	SAE	BRNN
Number of values	20	20	20	20	20
Minimum	0.003429	0.4126	0.2372	0.3786	0.2014
25% Percentile	0.003729	0.5126	0.3372	0.4786	0.2446
Median	0.003729	0.5126	0.3372	0.4786	0.2446
75% Percentile	0.003729	0.5126	0.3372	0.4786	0.2446
Maximum	0.003829	0.6713	0.4937	0.5786	0.2946
Range	0.0004	0.2587	0.2565	0.2	0.09316
10% Percentile	0.003639	0.4934	0.3372	0.4156	0.2356
90% Percentile	0.003729	0.5126	0.3822	0.4786	0.2716
Mean	0.003714	0.5145	0.3425	0.4751	0.2459
Std. Deviation	0.00007452	0.04326	0.04379	0.03602	0.01674
Std. Error of Mean	0.00001666	0.009673	0.009792	0.008055	0.003744
Coefficient of variation	2.006%	8.409%	12.79%	7.582%	6.808%
Geometric mean	0.003713	0.5129	0.34	0.4738	0.2454
Geometric SD factor	1.021	1.083	1.131	1.08	1.07
Harmonic mean	0.003712	0.5113	0.3376	0.4724	0.2449
Quadratic mean	0.003715	0.5162	0.3452	0.4764	0.2465
Skewness	-3.136	2.012	1.654	-0.1042	0.6119
Kurtosis	12.45	11.15	9.226	5.943	5.853
Sum	0.07428	10.29	6.85	9.503	4.919

TABLE 18. ANOVA test results for wind speed forecasting using the presented algorithm and other deep learning techniques over 20 runs.

	SS	DF	MS	F (DFn, DFd)	P value
Between columns, Treatment	3.357	4	0.8392	F (4, 95) = 781.8	P < 0.0001
Within columns, Residual	0.102	95	0.001073	-	-
Total	3.459	99	-	-	-

TABLE 19. Wilcoxon signed rank test of wind speed forecasting results using the presented algorithm and other deep learning techniques over 20 runs.

	ADPSO-Guided WOA	TDNN	DNN	SAE	BRNN
Theoretical median	0	0	0	0	0
Actual median	0.003729	0.5126	0.3372	0.4786	0.2446
# Values	20	20	20	20	20
Wilcoxon Signed Rank Test					
Sum of Signed ranks (W)	210	210	210	210	210
Positive ranks, Sum	210	210	210	210	210
Negative ranks, Sum	0	0	0	0	0
P value (two tailed)	0.0001	0.0001	0.0001	0.0001	0.0001
Estimate or Exact?	Exact	Exact	Exact	Exact	Exact
Summary of P value	****	****	****	****	****
Significant (alpha=0.05)?	Yes	Yes	Yes	Yes	Yes
How big is the discrepancy?					
Discrepancy	0.003729	0.5126	0.3372	0.4786	0.2446

other deep learning techniques. The results in the table show that the proposed optimizing ensemble model with MAPE of (1.8755), MAE of (0.00476), RMSE of (0.003728832), RRMSE of (1.279369489), and r of (0.9998878) gives competitive results compared to the TDNN, DNN, SAE, and BRNN techniques for the wind speed forecasting

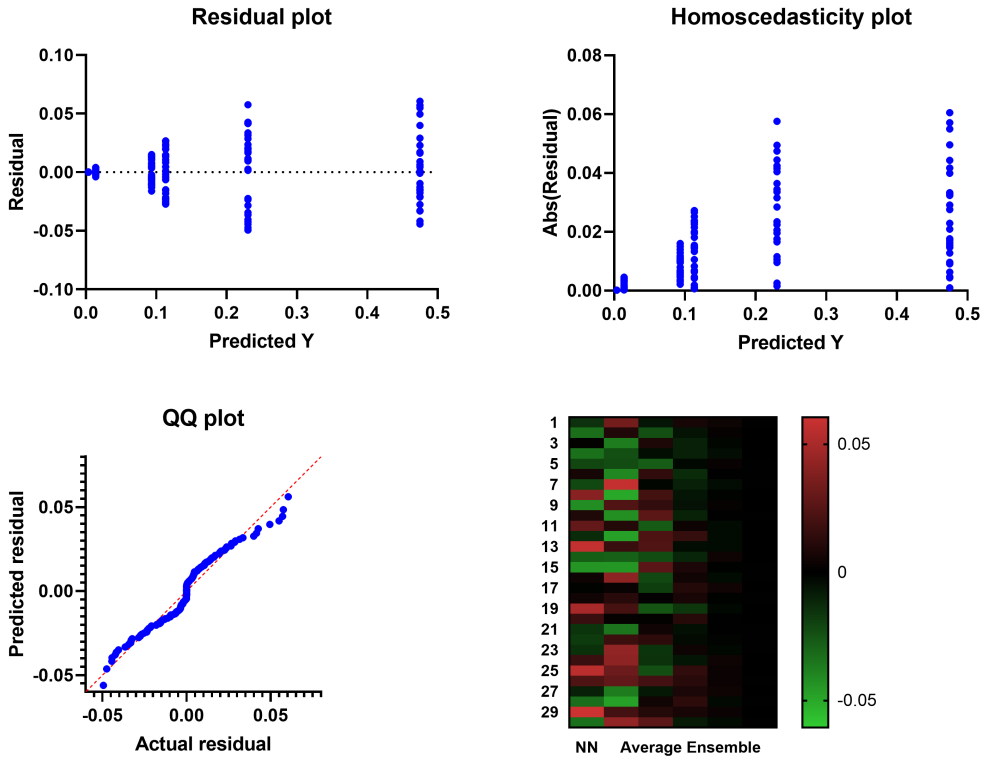

FIGURE 13. Residual, QQ, heteroscedasticity plots, and the heat map of the presented ensemble-based and compared models for wind speed forecasting problem.

tested problem. Table 17 shows the proposed algorithm's descriptive statistics compared to other deep learning techniques over 20 runs.

The ANOVA test results for wind speed forecasting based on the proposed algorithm compared to other deep learning techniques is shown in Table 18. The test of the Wilcoxon Signed-Rank rest of the wind speed forecasting results based on the proposed algorithm compared to other deep learning techniques is also shown in Table 19. The results confirm the superiority of the AD-PSO-Guided WOA based proposed ensemble model and indicate the statistical significance of the algorithm for the wind speed forecasting tested problem compared to the TDNN, DNN, SAE, and BRNN techniques.

V. CONCLUSION

This paper uses a dataset of wind power forecasting as a case study from Kaggle to predict hourly power generation up to forty-eight hours ahead at seven wind farms. A proposed adaptive dynamic particle swarm algorithm with a guided whale optimization algorithm improves the forecasting performance of the tested dataset by enhancing the parameters of the LSTM classification method. The AD-PSO-Guided WOA algorithm selects the optimal hyper-parameters value of the LSTM deep learning model for forecasting purposes of wind speed. A binary AD-PSO-Guided WOA algorithm is applied for feature selection and it is evaluated in comparison with the GWO, PSO, SFS, WOA, FA, and GA algorithms using the tested dataset. An optimized ensemble method based on the proposed algorithm is tested on the experiments' dataset. The results of this scenario are compared with NN, RF, LSTM, Average ensemble, and k-NN methods. The statistical analysis of different tests is performed to confirm the accuracy of the algorithm, including ANOVA and Wilcoxon's rank-sum tests. The current work's importance is applying a new optimization algorithm to enhance LSTM classifier parameters. The presented algorithms will be tested for other datasets in future work. The algorithm will also be tested for other binary problems for the constrained engineering, classification, and feature selection problems. The sparsity of the proposed model will be evaluated and compared with other methods including the sparse autoencoding methods.

REFERENCES

[1] M. Santhosh, C. Venkaiah, and D. M. V. Kumar, "Current advances and approaches in wind speed and wind power forecasting for improved renewable energy integration: A review," *Eng. Rep.*, vol. 2, no. 6, May 2020, Art. no. e12178, doi: 10.1002/eng2.12178.

[2] B. Kosovic, S. E. Haupt, D. Adriaansen, S. Alessandrini, G. Wiener, L. D. Monache, Y. Liu, S. Linden, T. Jensen, W. Cheng, M. Politovich, and P. Prestopnik, "A comprehensive wind power forecasting system integrating artificial intelligence and numerical weather prediction," *Energies*, vol. 13, no. 6, p. 1372, Mar. 2020, doi: 10.3390/en13061372.

[3] Z. Lin, X. Liu, and M. Collu, "Wind power prediction based on high-frequency SCADA data along with isolation forest and deep learning neural networks," *Int. J. Electr. Power Energy Syst.*, vol. 118, Jun. 2020, Art. no. 105835, doi: 10.1016/j.ijepes.2020.105835.

[4] M. Ibrahim, A. Alsheikh, Q. Al-Hindawi, S. Al-Dahidi, and H. ElMoaqet, "Short-time wind speed forecast using artificial learning-based algorithms," *Comput. Intell. Neurosci.*, vol. 2020, pp. 1–15, Apr. 2020, doi: 10.1155/2020/8439719.

[5] J. M. Lima, A. K. Guetter, S. R. Freitas, J. Panetta, and J. G. Z. de Mattos, "A meteorological–statistic model for short-term wind power forecasting," *J. Control, Autom. Electr. Syst.*, vol. 28, no. 5, pp. 679–691, Jul. 2017, doi: 10.1007/s40313-017-0329-8.

[6] J. Liu, X. Wang, and Y. Lu, "A novel hybrid methodology for short-term wind power forecasting based on adaptive neuro-fuzzy inference system," *Renew. Energy*, vol. 103, pp. 620–629, Apr. 2017, doi: 10.1016/j.renene.2016.10.074.

[7] M. Khodayar, J. Wang, and M. Manthouri, "Interval deep generative neural network for wind speed forecasting," *IEEE Trans. Smart Grid*, vol. 10, no. 4, pp. 3974–3989, Jul. 2019, doi: 10.1109/TSG.2018.2847223.

[8] M. Khodayar, O. Kaynak, and M. E. Khodayar, "Rough deep neural architecture for short-term wind speed forecasting," *IEEE Trans. Ind. Informat.*, vol. 13, no. 6, pp. 2770–2779, Dec. 2017, doi: 10.1109/TII.2017.2730846.

[9] M. Khodayar and J. Wang, "Spatio-temporal graph deep neural network for short-term wind speed forecasting," *IEEE Trans. Sustain. Energy*, vol. 10, no. 2, pp. 670–681, Apr. 2019, doi: 10.1109/TSTE.2018.2844102.

[10] S. M. J. Jalali, S. Ahmadian, M. Khodayar, A. Khosravi, V. Ghasemi, M. Shafie-Khah, S. Nahavandi, and J. P. S. Catalão, "Towards novel deep neuroevolution models: Chaotic levy grasshopper optimization for short-term wind speed forecasting," *Eng. Comput.*, vol. 2021, pp. 1–25, Mar. 2021, doi: 10.1007/s00366-021-01356-0.

[11] H. S. Dhiman, D. Deb, and J. M. Guerrero, "Hybrid machine intelligent SVR variants for wind forecasting and ramp events," *Renew. Sustain. Energy Rev.*, vol. 108, pp. 369–379, Jul. 2019, doi: 10.1016/j.rser.2019.04.002.

[12] H. S. Dhiman and D. Deb, "Machine intelligent and deep learning techniques for large training data in short-term wind speed and ramp event forecasting," *Int. Trans. Electr. Energy Syst.*, Feb. 2021, Art. no. e12818, doi: 10.1002/2050-7038.12818.

[13] H. S. Dhiman, D. Deb, S. M. Muyeen, and I. Kamwa, "Wind turbine gearbox anomaly detection based on adaptive threshold and twin support vector machines," *IEEE Trans. Energy Convers.*, early access, Apr. 27, 2021, doi: 10.1109/TEC.2021.3075897.

[14] B. Bilal, M. Ndongo, K. H. Adjallah, A. Sava, C. M. F. Kebe, P. A. Ndiaye, and V. Sambou, "Wind turbine power output prediction model design based on artificial neural networks and climatic spatiotemporal data," in *Proc. IEEE Int. Conf. Ind. Technol. (ICIT)*, Feb. 2018, pp. 1085–1092, doi: 10.1109/ICIT.2018.8352329.

[15] J. Wang, W. Yang, P. Du, and Y. Li, "Research and application of a hybrid forecasting framework based on multi-objective optimization for electrical power system," *Energy*, vol. 148, pp. 59–78, Apr. 2018, doi: 10.1016/j.energy.2018.01.112.

[16] Y.-Y. Hong, C. L. Paulo, and P. Rioflorido, "A hybrid deep learning-based neural network for 24-h ahead wind power forecasting," *Appl. Energy*, vol. 250, no. 15, pp. 530–539, Sep. 2019, doi: 10.1016/j.apenergy.2019.05.044.

[17] J. Zhang, J. Yan, D. Infield, Y. Liu, and F.-S. Lien, "Short-term forecasting and uncertainty analysis of wind turbine power based on long short-term memory network and Gaussian mixture model," *Appl. Energy*, vol. 241, pp. 229–244, May 2019, doi: 10.1016/j.apenergy.2019.03.044.

[18] E.-S. M. El-Kenawy and M. Eid, "Hybrid gray wolf and particle swarm optimization for feature selection," *Int. J. Innov. Comput. Inf. Control*, vol. 16, no. 3, pp. 831–844, 2020.

[19] R. Bello, Y. Gomez, A. Nowe, and M. M. Garcia, "Two-step particle swarm optimization to solve the feature selection problem," in *Proc. 7th Int. Conf. Intell. Syst. Design Appl. (ISDA)*, Oct. 2007, pp. 691–696.

[20] E.-S. M. El-Kenawy, A. Ibrahim, S. Mirjalili, M. M. Eid, and S. E. Hussein, "Novel feature selection and voting classifier algorithms for COVID-19 classification in CT images," *IEEE Access*, vol. 8, pp. 179317–179335, 2020, doi: 10.1109/ACCESS.2020.3028012.

[21] S. Mirjalili and A. Lewis, "The whale optimization algorithm," *Adv. Eng. Softw.*, vol. 95, pp. 51–67, May 2016. [Online]. Available: http://www.sciencedirect.com/science/article/pii/S0965997816300163

[22] E. M. Hassib, A. I. El-Desouky, L. M. Labib, and E.-S.-M. El-Kenawy, "WOA + BRNN: An imbalanced big data classification framework using whale optimization and deep neural network," *Soft Comput.*, vol. 24, no. 8, pp. 5573–5592, Mar. 2019, doi: 10.1007/s00500-019-03901-y.

[23] M. M. Kabir, M. Shahjahan, and K. Murase, "A new local search based hybrid genetic algorithm for feature selection," *Neurocomputing*, vol. 74, no. 17, pp. 2914–2928, 2011. [Online]. Available: http://www.sciencedirect.com/science/article/pii/S0925231211002748

[24] I. Fister, Jr., X.-S. Yang, I. Fister, and J. Brest, "Memetic firefly algorithm for combinatorial optimization," 2012, *arXiv:1204.5165*. [Online]. Available: http://arxiv.org/abs/1204.5165

[25] A. A. Heidari, S. Mirjalili, H. Faris, I. Aljarah, M. Mafarja, and H. Chen, "Harris hawks optimization: Algorithm and applications," *Future Gener. Comput. Syst.*, vol. 97, pp. 849–872, Aug. 2019, doi: 10.1016/j.future.2019.02.028.

[26] A. Ibrahim, H. A. Ali, M. M. Eid, and E.-S.-M. El-Kenawy, "Chaotic Harris hawks optimization for unconstrained function optimization," in *Proc. 16th Int. Comput. Eng. Conf. (ICENCO)*, Dec. 2020, pp. 153–158, doi: 10.1109/ICENCO49778.2020.9357403.

[27] S. Li, H. Chen, M. Wang, A. A. Heidari, and S. Mirjalili, "Slime mould algorithm: A new method for stochastic optimization," *Future Gener. Comput. Syst.*, vol. 111, pp. 300–323, Oct. 2020, doi: 10.1016/j.future.2020.03.055.

[28] A. Faramarzi, M. Heidarinejad, S. Mirjalili, and A. H. Gandomi, "Marine predators algorithm: A nature-inspired metaheuristic," *Expert Syst. Appl.*, vol. 152, Aug. 2020, Art. no. 113377, doi: 10.1016/j.eswa.2020.113377.

[29] M. Khishe and M. R. Mosavi, "Chimp optimization algorithm," *Expert Syst. Appl.*, vol. 149, Jul. 2020, Art. no. 113338, doi: 10.1016/j.eswa.2020.113338.

[30] F. Noman, G. Alkawsi, A. A. Alkahtani, A. Q. Al-Shetwi, S. K. Tiong, N. Alalwan, J. Ekanayake, and A. I. Alzahrani, "Multistep short-term wind speed prediction using nonlinear auto-regressive neural network with exogenous variable selection," *Alexandria Eng. J.*, vol. 60, no. 1, pp. 1221–1229, Feb. 2021, doi: 10.1016/j.aej.2020.10.045.

[31] X. Liu, H. Zhang, X. Kong, and K. Y. Lee, "Wind speed forecasting using deep neural network with feature selection," *Neurocomputing*, vol. 397, pp. 393–403, Jul. 2020, doi: 10.1016/j.neucom.2019.08.108.

[32] T. Su, Y. Liu, J. Zhao, and J. Liu, "Probabilistic stacked denoising autoencoder for power system transient stability prediction with wind farms," *IEEE Trans. Power Syst.*, vol. 36, no. 4, pp. 3786–3789, Jul. 2021, doi: 10.1109/TPWRS.2020.3043620.

[33] J. F. Torres, D. Hadjout, A. Sebaa, F. Martínez-Álvarez, and A. Troncoso, "Deep learning for time series forecasting: A survey," *Big Data*, vol. 9, no. 1, pp. 3–21, Feb. 2021, doi: 10.1089/big.2020.0159.

[34] M. S. Nazir, F. Alturise, S. Alshmrany, H. M. J. Nazir, M. Bilal, A. N. Abdalla, P. Sanjeevikumar, and Z. M. Ali, "Wind generation forecasting methods and proliferation of artificial neural network: A review of five years research trend," *Sustainability*, vol. 12, no. 9, p. 3778, May 2020, doi: 10.3390/su12093778.

[35] E.-S. M. El-Kenawy, S. Mirjalili, A. Ibrahim, M. Alrahmawy, M. El-Said, R. M. Zaki, and M. M. Eid, "Advanced meta-heuristics, convolutional neural networks, and feature selectors for efficient COVID-19 X-ray chest image classification," *IEEE Access*, vol. 9, pp. 36019–36037, 2021, doi: 10.1109/ACCESS.2021.3061058.

[36] A. A. Nasser, M. Z. Rashad, and S. E. Hussein, "A two-layer water demand prediction system in urban areas based on micro-services and LSTM neural networks," *IEEE Access*, vol. 8, pp. 147647–147661, 2020, doi: 10.1109/ACCESS.2020.3015655.

[37] S. S. M. Ghoneim, T. A. Farrag, A. A. Rashed, E.-S. M. El-Kenawy, and A. Ibrahim, "Adaptive dynamic meta-heuristics for feature selection and classification in diagnostic accuracy of transformer faults," *IEEE Access*, vol. 9, pp. 78324–78340, 2021, doi: 10.1109/ACCESS.2021.3083593.

[38] S. Mirjalili, S. M. Mirjalili, S. Saremi, and S. Mirjalili, "Whale optimization algorithm: Theory, literature review, and application in designing photonic crystal filters," *Nature-Inspired Optimizers*. Cham, Switzerland: Springer, 2020, pp. 219–238, doi: 10.1007/978-3-030-12127-3_13.

[39] *Global Energy Forecasting Competition 2012—Wind Forecasting*. Accessed: Jun. 19, 2021. [Online]. Available: https://www.kaggle.com/c/GEF2012-wind-forecasting

[40] R. Al-Hajj, A. Assi, and M. M. Fouad, "Stacking-based ensemble of support vector regressors for one-day ahead solar irradiance prediction," in *Proc. 8th Int. Conf. Renew. Energy Res. Appl. (ICRERA)*, Nov. 2019, pp. 428–433, doi: 10.1109/ICRERA47325.2019.8996629.

ABDELHAMEED IBRAHIM (Member, IEEE) received the bachelor's and master's degrees in engineering from the Computer Engineering and Systems Department, in 2001 and 2005, respectively, and the Ph.D. degree in engineering from the Faculty of Engineering, Chiba University, Japan, in 2011. He was with the Faculty of Engineering, Mansoura University, Egypt, from 2001 to 2007, where he is currently an Associate Professor of computer engineering. He has published over 50 publications with over 1000 citations and an H-index of 19. His research interests include machine learning, optimization, swarm intelligence, and pattern recognition. He serves as a Reviewer for *Journal of Electronic Imaging*, IEEE Access, *Computer Standards and Interfaces*, *Optical Engineering*, IEEE Journal of Biomedical and Health Informatics, *Biomedical Signal Processing and Control*, *IET Image Processing*, *Multimedia Tools and Applications*, *Frontiers of Information Technology & Electronic Engineering*, *Journal of Healthcare Engineering*, and other respected journals.

SEYEDALI MIRJALILI (Senior Member, IEEE) is currently the Director of the Centre for Artificial Intelligence Research and Optimization, Torrens University Australia, Brisbane. He has published over 200 publications with over 36,000 citations and an H-index of 65. As the most cited researcher in robust optimization, he is in the list of 1% highly cited researchers and named as one of the most influential researchers in the world by the Web of Science. He is also internationally recognized for his advances in swarm intelligence and optimization, including the first set of algorithms from a synthetic intelligence standpoint—a radical departure from how natural systems are typically understood—and a systematic design framework to reliably benchmark, evaluate, and propose computationally cheap robust optimization algorithms. He is also working on the applications of multi-objective and robust meta-heuristic optimization techniques as well. His research interests include robust optimization, engineering optimization, multi-objective optimization, swarm intelligence, evolutionary algorithms, and artificial neural networks. He is also an Associate Editor of several journals, including *Applied Soft Computing*, *Neurocomputing*, *Applied Intelligence*, *Advances in Engineering Software*, IEEE Access, and *PLOS One*.

M. EL-SAID received the B.Sc. (Hons.), M.Sc., and Ph.D. degrees in electric power engineering from Mansoura University, Egypt, in 1981, 1987, and 1992, respectively. He is currently the Dean of the Delta Higher Institute of Engineering and Technology, Ministry of Higher Education, Egypt. He is also an Official Reviewer for Egyptian Universities Promotion Committees—Supreme Council of Universities in Egypt. He has been a Professor of electric power systems with the Department of Electrical Engineering, Faculty of Engineering, Mansoura University, since 2005. He was the Vice-Dean of the Community Services and Environmental Development, Faculty of Engineering, Mansoura University, from 2010 to 2011. He was also the Director of the Communication and Information Technology Centre (CITC), Mansoura University, from 2014 to 2016. From 2016 to 2018, he was the Dean of the Faculty of Engineering, Mansoura University. His research interests include renewable energy, smart grids, and power system operation and control. He is also a Reviewer of scientific journals, including *Electric Power Components and Systems*, IEEE Transactions on Power Systems, and IEEE Transactions on Power Delivery.

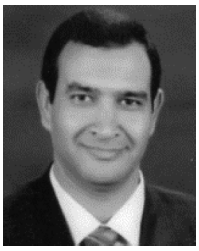

SHERIF S. M. GHONEIM (Senior Member, IEEE) received the B.Sc. and M.Sc. degrees from the Faculty of Engineering at Shoubra, Zagazig University, Egypt, in 1994 and 2000, respectively, and the Ph.D. degree in electrical power and machines from the Faculty of Engineering, Cairo University, in 2008. Since 1996, he has been teaching with the Faculty of Industrial Education, Suez Canal University, Egypt. From 2005 to 2007, he was a Guest Researcher with the Institute of Energy Transport and Storage (ETS), University of Duisburg–Essen, Germany. He joined the Electrical Engineering Department, Faculty of Engineering, Taif University, as an Associate Professor. His research interests include grounding systems, breakdown in SF6 gas, dissolved gas analysis, and AI technique applications.

MOSLEH M. AL-HARTHI was born in Taif, Saudi Arabia, in October 1966. He received the B.Sc. and M.S. degrees in electronics technology and engineering from Indiana State University, Terre Haute, USA, in 1996 and 1997, respectively, and the Ph.D. degree in electrical engineering from Arkansas University, Fayetteville, USA, in 2001. He was an Assistant Professor with the College of Technology, Jeddah, Saudi Arabia, from 2001 to 2009. He is currently working as an Associate Professor with the Electrical Engineering Department, Taif University, Saudi Arabia. His research interests include electronics, control engineering, and signal processing.

TAREK F. IBRAHIM received the Ph.D. degree in pure mathematics from the Faculty of Science, Mansoura University, Egypt, in 2006. He is currently an Associate Professor of pure mathematics. He has published over 47 publications with over 538 citations and an H-index of 14. His research interests include difference equations and their topics in engineering and physics. He serves as a Reviewer for many international journals, such as *Mathematical Problems in Engineering*, *Mathematical Methods in the Applied Sciences*, *British Journal of Mathematics & Computer Science*, and other respected journals.

EL-SAYED M. EL-KENAWY (Member, IEEE) is currently an Assistant Professor with the Delta Higher Institute for Engineering and Technology (DHIET), Mansoura, Egypt. He published more than 35 articles with more than 750 citations and an H-index of 19. He has launched and pioneered independent research programs. He is also motivating and inspiring his students by different ways by providing a thorough understanding of a variety of computer concepts and explains complex concepts in an easy-to-understand manner. His research interests include artificial intelligence, machine learning, optimization, deep learning, digital marketing, and data science. He is also a Reviewer for *Computers, Materials & Continua* journal, IEEE Access, and some other journals.